

## OPACITY SAMPLING IN RADIATIVE ACCELERATION CALCULATIONS

F. LEBLANC

Département de physique, Université de Moncton, Moncton, N.-B., Canada E1A 3E9; leblanf@UMoncton.CA

AND

G. MICHAUD<sup>1</sup> AND J. RICHER<sup>1</sup>

Département de physique et d'astronomie, Université de Montréal, Montréal, PQ, Canada, H3C 3J7; Georges.Michaud@CERCA.UMontreal.CA,  
Jacques.Richer@CERCA.UMontreal.CA

Received 1999 November 19; accepted 2000 March 2

### ABSTRACT

The accuracy requirements on atomic data for the calculation of stellar evolution with atomic diffusion are determined. In particular, the density of frequency grids needed for precise radiative acceleration ( $g_{\text{rad}}$ ) calculations via the sampling method are presented. In order to minimize the number of frequency points needed for precise  $g_{\text{rad}}$  calculations, frequency grids that are more refined in the regions of the spectrum where the radiative flux is large are suggested. The following number of frequency points are needed for opacity table calculations to be used in stellar evolutionary codes including diffusion: 50,000 points for  $4.20 \leq \log T \leq 4.5$ , 30,000 points for  $4.5 < \log T \leq 4.8$ , 10,000 points for  $4.8 < \log T \leq 5.5$ , and 4000 points for  $\log T > 5.5$ . These opacity tables would render possible the study atomic diffusion in the exterior regions of certain chemically peculiar stars such as Ap or HgMn stars. In the sampling method, correction factors can be applied after the basic integrations over sampled spectra to include such effects as ion velocity averaging, redistribution of momentum among ions, and electron recoil during photoionization; these corrections are evaluated and illustrated for a few typical stellar models. Silicon is used as an example to show that the corrections are important mainly for  $T < 50,000$  K. These corrections are used in stellar evolution calculations based on OPAL monochromatic opacity tables.

*Subject headings:* acceleration of particles — diffusion — stars: chemically peculiar

### 1. INTRODUCTION

Particle transport appears to play an important role in a large number of stars, from Bp stars to the Sun. In many objects (Ap stars, Bp stars, horizontal branch stars, etc.) momentum transfer to atoms via photoabsorption (Michaud 1970) dominates competing hydrodynamical processes in particle transport in stellar atmospheres and stellar interiors. It is then imperative to obtain precise radiative accelerations of the various elements in order to study the effect of diffusion on the structure and evolution of stars.

The availability of large atomic data banks has made it possible to introduce radiative accelerations self consistently with evolution (Richer et al. 1998). As the abundance of chemical species varies locally, the Rosseland opacity can be computed consistently with the local time-dependent abundances. The radiative accelerations are calculated simultaneously taking into account all changes in the background opacity. For that purpose all species contributing to opacity at the line frequency must be included in the calculations; ideally, the frequency of each line should be known accurately. The radiative forces drive particle transport and lead to large structural changes through the appearance of iron peak convection zones in F and A stars (Turcotte, Richer, & Michaud 1998a; Richer et al. 2000; J. Richer, G. Michaud, & O. Richard 2000, in preparation).

The calculations of Turcotte et al. (1998a) were limited to relatively cool F stars partly because of limitations of the OPAL (Rogers & Iglesias 1992a, 1992b; Iglesias & Rogers 1995, 1996) data to calculate radiative accelerations. In particular, while the opacity sampling they use has sufficient

resolution to calculate Rosseland opacities, it is not sufficient to calculate radiative accelerations for less abundant species in the outer stellar regions (Richer et al. 1998). Richer, Michaud, & Turcotte (2000) conclude that while in AmFm stars chemical separation probably occurs mainly below the iron peak convection zone, there are stars where the separation occurs in more superficial regions. For instance the very large abundance anomalies observed in HgMn stars can probably be explained only by separation right up to the atmosphere. Even if HgMn stars have Fe peak convection zones, these may not mix the whole region above them completely in the absence of H and He convection zones. It is then important to determine what are the accuracy requirements for  $g_{\text{rad}}$  calculations in such low temperature regions.

The aim of this paper is to determine the required frequency resolution and then to find the minimum number of mesh points in  $u$  ( $\equiv hv/kT$ ) needed, as a function of temperature, to obtain precise radiative accelerations to study the effect of atomic diffusion on the evolution of stars of various masses. The radiative acceleration shown here have been obtained using the Opacity Project (hereafter OP) data (Seaton 1987; Seaton et al. 1992) obtained via TOPbase (Cunto et al. 1993), except for Fe I and Fe II, where the Kurucz (1990, 1991) line data was used. We will also compare the  $g_{\text{rad}}$  calculated here to those obtained by the method described in Gonzalez et al. (1995b, hereafter GLAM) and in Seaton (1997). The importance of ion averaging, redistribution of momentum among ions, and electron recoil during photoionization will also be evaluated; these effects are generally *not* included in the spectra and must be added separately.

Note that although there will be frequent references in the following to OPAL data and  $g_{\text{rad}}$  calculations based on

<sup>1</sup> Centre de Recherche en Calcul Appliqué (CERCA), 5160 boulevard Décarie, bureau 400, Montréal, PQ, Canada H3X 2H9.

OPAL spectra, these data were not used in the calculations done for this paper. The results of the present study should be useful for the creation of the next generation of OPAL-like monochromatic opacity tables.

## 2. RADIATIVE ACCELERATION CALCULATIONS

The radiative acceleration  $g_{\text{rad}}(A)$  on an element  $A$  at radius  $r$  in a star may be approximated (at large optical depths) by

$$g_{\text{rad}}(A) = \frac{1}{4\pi r^2} \frac{L_r^{\text{rad}}}{c} \frac{\kappa_r}{X_A} \int_0^\infty \frac{\kappa_u(A)}{\kappa_u(\text{total})} \mathcal{P}(u) du, \quad (1)$$

and  $\mathcal{P}(u)$  is the normalized flux distribution:

$$\mathcal{P}(u) \equiv \frac{15}{4\pi^4} \frac{u^4 e^u}{(e^u - 1)^2}. \quad (2)$$

The radiative luminosity at radius  $r$  is  $L_r^{\text{rad}}$ ,  $\kappa_r$  is the Rosseland opacity,  $\kappa_u(\text{total})$  is the total opacity at the frequency point defined by  $u$ , and  $X_A$  is the mass fraction of the element under consideration. The value of  $g_{\text{rad}}$  depends on the competition for photons between the element  $A$  and the other elemental species present. Knowledge of the atomic data of all of these elements is therefore needed to evaluate  $g_{\text{rad}}$  for a given species.

Opacity Project (Seaton 1987; Seaton et al. 1992) and Kurucz (1990, 1991) data have been used to calculate the radiative accelerations of various elements including CNO (Gonzalez, Artru, & Michaud 1995a; Seaton 1997), Al (Hui-Bon-Hoa et al. 1996; Seaton 1997) and Fe (Alecian, Michaud, & Tully 1993; LeBlanc & Michaud 1995; Seaton 1997, 1999). The various methods used in these studies to obtain  $g_{\text{rad}}$  and the tabulation of Rosseland opacities as a function of  $X$ ,  $Y$ , and  $Z$ , do not permit taking into account the effect of abundance changes on the structure of the models nor of the abundance change of one species on the  $g_{\text{rad}}$  of another. This requires taking into account metal abundance changes in more detail than the simple  $Z$ -dependence allows.

In order to evaluate  $g_{\text{rad}}$  at a given temperature and pressure we can calculate an opacity spectrum for each element on a certain frequency grid and then integrate equation (1). This is commonly called the *opacity sampling* method. In the method used by GLAM, where the contribution of each transition is integrated semianalytically, the total opacity is divided into two parts prior to each line profile integration: the opacity of the transition under consideration, and the rest of the spectrum, called the background opacity for that line, which is then approximated by a simple constant (that is, independent of  $u$ ; see GLAM and Richer et al. [1998] for more details). GLAM calculated opacities in 4000 evenly spaced intervals of width  $\Delta u = 0.005$  for  $0 < u \leq 20$ . For the background opacity the bound-bound cross-sections ( $\pi e^2 f / m_e c$ , where  $f$  is the oscillator strength of the transition) were evenly distributed in the  $\Delta u$  interval that contained the natural frequency of the line. In previous  $g_{\text{rad}}$  calculations (Alecian et al. 1993; Borsenberger, Michaud, & Praderie 1979; Borsenberger, Praderie, & Michaud 1981) a simple formula scaled with the Rosseland mean (Borsenberger et al. 1979) was used for the background opacity. In stellar evolution codes GLAM suggested the use of  $g_{\text{rad}}$  interpolation tables. But this method has the disadvantage that during evolutionary model calculations the effect of the simultaneous changes in the abundances of the various ele-

ments cannot be included in the radiative acceleration calculations. However, the method developed by GLAM allowed calculating Rosseland opacities during evolution, and so the effect of abundance variations on stellar structure.

Alecian (1985) and Alecian & Artru (1990) developed a method whereby  $g_{\text{rad}}$  due to bound-bound transitions is obtained via an approximate equation that is defined by two parameters for each ion. This method has the advantage that no frequency integration is needed and is therefore very efficient numerically. However, as for  $g_{\text{rad}}$  tables, it cannot take into account the effects on  $g_{\text{rad}}$  of chemical composition variations caused by the diffusion of the various elements during evolution. Alecian (1994) also developed an approximate equation for  $g_{\text{rad}}$  due to photoionization, but this method is not valid for abundant elements such as CNO or Fe.

Richer et al. (1998) calculated  $g_{\text{rad}}$  using the opacity sampling method with OPAL spectra. These calculations were done during stellar evolution simulations of F-type stars (Turcotte et al. 1998a) and the Sun (Turcotte et al. 1998b) that included atomic diffusion of 28 species. It was shown that the frequency grid used in the OPAL spectra is too coarse to obtain precise  $g_{\text{rad}}$  in outer stellar regions. At these lower temperatures the atomic line widths are small, thus more frequency points are needed to accurately sample these lines. At higher temperatures the grid used by OPAL was sufficient since the lines are broader.

Seaton (1997) also found that the use of a uniform grid containing  $10^4$  points was not sufficient for precise  $g_{\text{rad}}$  calculations at low temperatures. In that study the  $g_{\text{rad}}$  of 15 elements were calculated using the opacity sampling method with an evenly spaced  $10^5$  point frequency grid in  $u$  and  $g_{\text{rad}}$  interpolation tables were built. It is in that form that Seaton's results will be compared to other calculations in this paper.

The calculations presented here included the bound-bound and bound-free transitions of elements H, He, C, N, O, Ne, Mg, Si, S, Ar, and Fe given in the OP data base (Seaton 1987; Seaton et al. 1992; Cunto et al. 1993), except for Fe I and Fe II, where the Kurucz (1990, 1991) data was used. Thompson scattering was also included in the opacity spectrum calculations. The formalism of Hummer & Mihalas (1988) was used to calculate atomic populations.

## 3. RESOLUTION REQUIREMENTS IN STELLAR MODELS

The resolution in frequency that is required to accurately calculate radiative accelerations varies with temperature and density within a star. *The requirements are much more severe than for Rosseland mean opacity computations.* In this section, we describe the precision needed to properly calculate the effects of diffusion in F, A, and B stars, taking the likely mixing processes into account. The requirements are progressively more severe (1) if a large number of lines are involved, (2) when only a few lines contribute, and (3) when the detailed overlap of individual lines must be taken into account.

The appearance of fluctuations in the radiative accelerations as seen in Figures 1 and 2 of Richer et al. (1998) poses the problem of the limited frequency density of grids used in opacity calculations. Random fluctuations are seen in most chemical species at the lower temperatures ( $\sim 20,000$  K). Even at that low  $T$ , the fluctuations of the radiative accelerations of He, O, and Fe are perhaps acceptably small

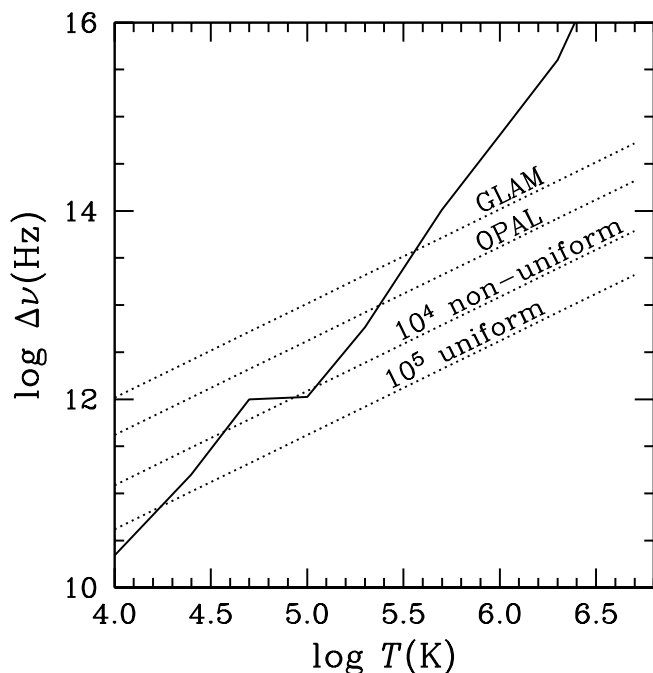


FIG. 1.—Variation of the average line widths of Mg transitions with  $gf > 1$  (solid line) in a typical A star [see § 4 for details concerning the  $(T, R_e)$  points chosen]. The dotted curves represent the frequency resolution (top to bottom) of the GLAM grid, the OPAL grid (an evenly spaced grid in  $u$  containing 10,000 points), a nonuniform grid with 10,000 points (see § 4 for details; the resolution given here is the average width of the intervals for  $3 < u < 6$ ), and an evenly spaced  $u$  grid with 100,000 points.

because either the large abundances imply broader lines (He and O) or the large number of lines implies contributions of a large number of frequency points (Fe). However, relatively large fluctuations are seen at  $T$  as high as 200,000 K in radiative acceleration of phosphorus, which has a small abundance and turns out to be in a configuration with very few spectral lines at that  $T$ . Consequently the OPAL data may be used with confidence for all elements so long as particle transport by atomic diffusion is important only at temperatures higher than 200,000 K. It may be used at lower temperatures so long as the results depend essentially on the most abundant elements (He, O, Fe, etc.).

In evolutionary calculations without turbulence or mass loss, for stars of mass less than  $1.4 M_{\odot}$ , the combined H and He convection zone always extends inward to temperatures higher than 200,000 K. The 10,000 point grid of OPAL is then sufficient. It turns out that in more massive stars without any mixing process, an iron peak convection zone always develops at  $T \sim 200,000$  K (Richer et al. 2000; J. Richer, et al. 2000, in preparation) so that the current OPAL grid is sufficient for the particle transport below that temperature. However, particle transport is important at lower temperatures before the iron peak convection zone develops in those models and if mixing by convection, turbulence, or some other process does not homogenize the regions at  $T < 200,000$  K. Furthermore, in HgMn stars very large overabundances of Hg ( $\sim 100,000$ ) are observed along with isotopic anomalies. Such large anomalies cannot develop below the iron convection zone since there is not sufficient time for that in the total evolutionary life of the star and, furthermore, there is probably not enough Hg in

the star to cause an overabundance by such a large factor for the whole mass in and above the iron convection zone. It will then be essential, in order to model HgMn stars, to study in detail the separation at cooler temperatures and probably in the atmosphere. If one is to study the isotope separation it will be essential to know which blends compete with the Hg lines for instance. It will then be necessary to determine the line position precisely and to calculate the lines with enough resolution. The atomic data determined using calculations cannot do that at the present time. The level positions are not known accurately enough to calculate blends of individual lines. Part of the HgMn star problem cannot be modeled with the present data. However, modeling HgMn stars sets an important goal for the development of atomic data banks.

In the atmosphere, the diffusion approximation used for the radiative flux in equation (1) is no longer valid. At these small optical depths the radiative transfer equation must be solved to obtain the flux precisely. Grids in  $u$  must then be abandoned since the radiative transfer equation has to be solved at given frequencies throughout the atmosphere. LeBlanc & LeBlanc (1999) found that approximately 200,000 frequency points are needed in such applications.

In between the complete solution of the HgMn stars, which requires detailed line overlap in the atmosphere, and the calculation of abundance anomalies in AmFm stars, which mainly requires separation at  $T > 200,000$  K, there remains the problem of the formation of the iron peak convection zone in AmFm and HgMn stars along with the potential explanation of some anomalies of the HgMn stars, in particular those involving the 28 species that are currently calculated with the OPAL data. The appearance of the iron peak convection zone depends on the diffusion of the most important contributors to opacity. These problems require the determination of radiative accelerations at temperatures between 20,000 and 200,000 K.

To calculate  $g_{\text{rad}}$  taking blends of individual lines into account, it is required to have a frequency grid spacing not larger than the Doppler width or the pressure width, whichever is larger. Figure 1 compares the average line widths of Mg lines with  $gf > 1$  at a few  $(T, R_e)$  points typical of stellar interiors ( $R_e \equiv N_e/T^3$ , in cgs units,  $N_e$  being the electron number density; see next section for more details) to the intervals of various frequency grids. Since one needs to cover the interval  $0 < u < 20$ , approximately 200,000 frequencies are required to evaluate  $g_{\text{rad}}$  accurately (when using an evenly spaced grid in  $u$ ) at  $T = 10^4$  K but less than 4000 frequencies at  $T = 10^6$  K. Consequently, since the OPAL opacities are calculated at  $10^4$  frequencies, the  $g_{\text{rad}}$  of Richer et al. (1998) are accurate for all chemical species at  $\log T \gtrsim 5.5$ , but as  $T$  is reduced they progressively lose accuracy. The  $g_{\text{rad}}$  of less abundant elements with the smallest number of lines become inaccurate first. This result is consistent with the preceding analysis of the  $g_{\text{rad}}$  by Richer et al. (1998). The requirements may be relaxed for very abundant elements as discussed above, but it is even more stringent if one wishes to study isotope anomalies where the detail of the interaction within each line is probably important.

As mentioned previously, Seaton (1997) used a uniform grid in  $u$  containing  $10^5$  points. Except for a few specific cases, for instance Ne at  $T = 10^4$  K, which has a relatively weak  $g_{\text{rad}}$ , we found that this grid is sufficiently fine to obtain precise  $g_{\text{rad}}$ .

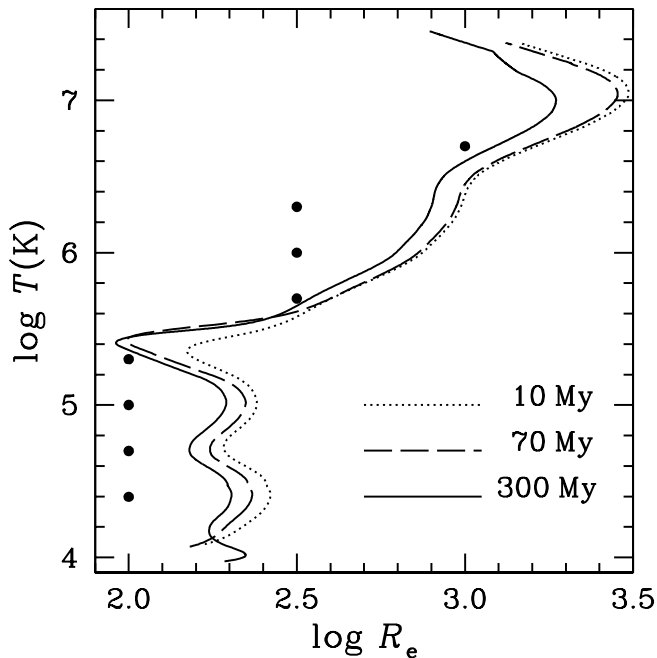


FIG. 2.—Paths of an evolving  $3 M_{\odot}$  stellar model in the  $(T, R_e)$  plane, at three different ages. Calculation points for this article are identified by filled circles.

#### 4. RADIATIVE FORCES BY OPACITY SAMPLING

To evaluate what gain in accuracy is achievable with a given number of frequency points, we opted to investigate grids that are more refined in the region where  $\mathcal{P}(u)$  (i.e., the radiative flux) is large (see Appendix A for details on how these grids were generated). These nonuniform grids have 3.4 times the number of points in the range  $u = 3-6$  (where  $\mathcal{P}(u)$  attains its maximum value) as compared to a uniform grid with the same total number of points; it was verified that they do give more accurate radiative accelerations than uniform grids with the same number of frequency points.<sup>2</sup>

Figure 2 shows paths in the  $(T, R_e)$  plane for the structure of a  $3 M_{\odot}$  star at different evolutionary stages, as calculated by Richer et al. (2000). We chose eight points in the  $(T, R_e)$  plane (*filled circles*) representative of the structure of this star; they are:  $(T = 25,000 \text{ K}, \log R_e = 2.0)$ ,  $(T = 50,000 \text{ K}, \log R_e = 2.0)$ ,  $(T = 100,000 \text{ K}, \log R_e = 2.0)$ ,  $(T = 200,000 \text{ K}, \log R_e = 2.0)$ ,  $(T = 500,000 \text{ K}, \log R_e = 2.5)$ ,  $(T = 1,000,000 \text{ K}, \log R_e = 2.5)$ ,  $(T = 2,000,000 \text{ K}, \log R_e = 2.5)$ , and  $(T = 5,000,000 \text{ K}, \log R_e = 3.0)$ . In Figure 1 a ninth point  $(T = 10,000 \text{ K}, \log R_e = 2.0)$  was also included. The values of  $R_e$  chosen here should somewhat overestimate the number of frequency points needed for  $g_{\text{rad}}$  calculations since, for a given  $T$ , the line widths increase with  $R_e$ .

In order to find nonuniform grids with the least number of points, the following procedure was used. We calculated the flux fraction  $F(A)$  absorbed by element  $A$ :

$$F(A) = \int_0^{\infty} \frac{\kappa_u(A)}{\kappa_u(\text{total})} \mathcal{P}(u) du, \quad (3)$$

<sup>2</sup> There are exceptions, however: if at some temperature an element absorbs mostly through a few narrow lines located at  $u \gtrsim 10$ , then the nonuniform grid result may be worse, because it has lower resolution than the corresponding uniform grid in that region. But in such a case, one expects  $g_{\text{rad}}$  to be relatively weak and unimportant.

at each of the above  $(T, R_e)$  points. This was done for each metal and for five different nonuniform grids with the same number of points. For instance, all the frequency points (except the first and last ones) of the nonuniform grid obtained by the method described in Appendix A were shifted by  $-0.01$ ,  $-0.005$ ,  $+0.005$ , and  $+0.01$  (in units of  $u$ ). Five opacity spectra were then calculated and used to obtain five values for  $F(A)$  for the various elements. Using several shifted grids for the same calculation allowed us to quantify the consequences of (effectively) random misalignment between narrow lines and grid points. It helped distinguishing good  $g_{\text{rad}}$  from accidentally good ones. These results were then compared to those calculated with a uniform grid with  $10^6$  points, for which the error on  $g_{\text{rad}}$  was verified to be less than 0.1%. The number of points of the nonuniform grids was varied until the desired accuracy was obtained.

Our aim is to obtain  $g_{\text{rad}}$  with an error not exceeding 0.1 dex for most elements, for abundances within a factor of 10 of the solar value. Since the number of frequency points needed to obtain accurate  $g_{\text{rad}}$  increases with decreasing abundance of the element in question, our calculations were performed using an abundance of 0.1 solar for the studied element, while the abundances of the other elements of the mixture were taken as solar. The solar abundances are taken from Grevesse, Noels, & Sauval (1992) and Grevesse & Noels (1993). Here is a summary of our results.

At  $T = 25,000 \text{ K}$ , the lowest temperature considered here, all of the elements except Mg, Ne, and Ar have an error of less than 0.1 dex down to an abundance of 0.1 solar for a grid using 30,000 points (see Fig. 3). Many have errors of less than 0.1 dex for abundances of  $\leq 0.01$  solar. When using a grid containing 50,000 points only Ne has an error of over 0.1 dex. At this temperature Ne is mostly in the F-like state, which has a relatively weak  $g_{\text{rad}}$  (see top of Fig. 3), and it would take a nonuniform grid with approximately  $10^5$  points to accurately sample the lines because they occupy only a small fraction of the spectrum. The choice of such a grid would greatly elongate evolutionary calculations and is not viable. But since the  $g_{\text{rad}}$  for a solar abundance of Ne in a star with  $T_{\text{eff}} = 10,000 \text{ K}$  is only a small fraction of surface gravity in main sequence stars, a larger relative error will not significantly affect the outcome of diffusion calculations. We thus suggest that a nonuniform grid with 50,000 points be used for this temperature.

At  $T = 50,000 \text{ K}$  all of the elements except Mg have an error of less than 0.1 dex down to an abundance of 0.1 solar for a grid with 30,000 points (no figure is shown). At this temperature Mg has a very weak  $g_{\text{rad}}$  because it is mostly in the Ne-like ionization state. We thus suggest that a nonuniform grid with 30,000 points be used for this temperature.

At  $T = 100,000 \text{ K}$  all of the elements except Si have an error of less than 0.1 dex down to an abundance of 0.1 solar for a grid with 10,000 points (see Fig. 4). At this temperature  $g_{\text{rad}}(\text{Si})$  is very weak because Si is mostly in the Ne-like ionization state. We thus suggest that a nonuniform grid with 10,000 points be used for this temperature. This conclusion is consistent with the results represented by the third dotted curve (from the top) of Figure 1, which shows that the resolution of this grid for  $3 < u < 6$  is of the same order as the average line widths.

Similar analyses were done for higher temperatures, and we concluded that nonuniform grids with the following number of points would give an accuracy better than

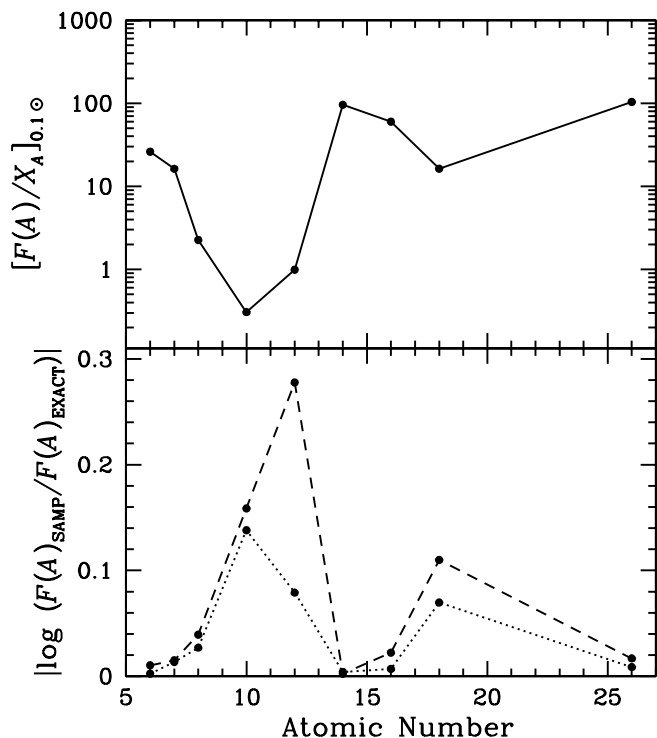


FIG. 3.— $F(A)/X_A$  for various elements at low concentration (*top*) and the relative error (*bottom*) on the fraction  $F(A)_{\text{SAMP}}$  of the flux absorbed by these elements when using nonuniform grids with 30,000 points (*dashed line*) and 50,000 points (*dotted line*), as compared to the results obtained on a uniform grid with  $10^6$  points [ $F(A)_{\text{EXACT}}$ ]. Calculations were done at  $T = 25,000$  K and  $\log R_e = 2.0$ , for a concentration of 0.1 solar for each element considered in turn, all the others then having solar concentrations.

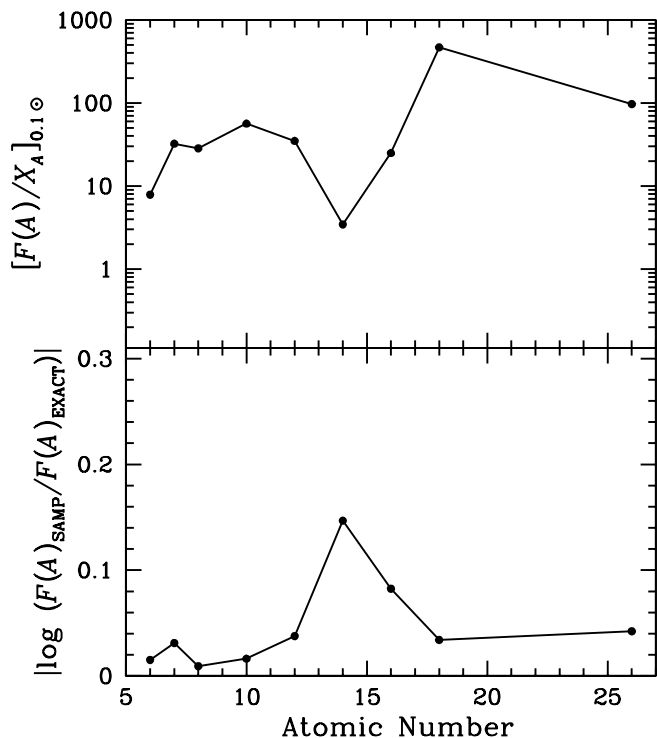


FIG. 4.—Same as Fig. 3 except that a 10,000 point nonuniform grid is used for  $F(A)_{\text{SAMP}}$  and the temperature is  $T = 100,000$  K.

$\sim 0.1$  dex for  $g_{\text{rad}}$  calculations: 50,000 points for  $4.20 \leq \log T \leq 4.5$ , 30,000 points for  $4.5 < \log T \leq 4.8$ , 10,000 points for  $4.8 < \log T \leq 5.5$ , and 4000 points for  $\log T > 5.5$ . At  $\log T \lesssim 4.20$  the lines become very narrow and it takes a larger number of points to accurately sample the opacity spectrum. The number of frequency points needed at these low temperatures can be estimated from Figure 1.

## 5. ROSSELAND MEAN OPACITIES

The Rosseland opacities were also obtained from the opacity spectra calculated on the proposed nonuniform frequency grids at the temperatures studied. These values were within 1% of the Rosseland mean calculated with a uniform grid with  $10^6$  points. Rosseland opacities obtained with monochromatic opacities calculated on the proposed frequency grids are then accurate enough to be used for stellar structure and evolution studies.

## 6. GLAM VERSUS OPACITY SAMPLING

In this section we shall compare  $F(A)$  for several elements using the opacity sampling method to the values obtained using the GLAM method, at the GLAM resolution. In both cases the same set of 11 elements was used to compose the total spectra. No redistribution of momentum among ions was included in either case and the diffusion coefficients of all ionization states were assumed equal.

A second goal of this section is to compare these results to those obtained using Seaton's (1997)  $g_{\text{rad}}$  interpolation tables.

As discussed in GLAM, the ionization state in which the acquired momentum is spent, after a bound-bound absorption for instance, may differ from the ionization state in which the photon was absorbed. This affects the value of the ion-averaged  $g_{\text{rad}}$  since the diffusion coefficient depends on the charge of the ion in which the momentum is spent. Since the sampling method is based on absorption spectra that are not weighted according to ionic diffusion coefficients (such weighting would have to be done on a line by line basis), it is best to leave this effect out of the present comparison. Moreover, we also neglected the fact that during photoionization a portion of the momentum can be transferred to the ejected electron. Richer, Michaud, & Massacrier (1997) showed that for Li the inclusion of the electron recoil formulas of Massacrier & El-Murr (1996) had only a small effect on  $g_{\text{rad}}$  of that element. Hui-Bon-Hoa et al. (1996) found similar results for Al using the H-like electron recoil formulas of Massacrier (1996). Since in the GLAM method a  $g_{\text{rad}}$  is calculated for each transition separately, effects such as redistribution and electron recoil can be included. In the sampling method these effects cannot be included directly since in order to be numerically viable only one opacity spectrum is handled for each element. Correction factors that include the physical processes mentioned above will be discussed in § 7.

In the GLAM calculations only H, He, C, N, O, and Fe were included; these authors then felt it necessary to correct the total monochromatic opacity used in equation (1) to take into account the opacity of the missing elements. This correction is not applied in the present calculations since more metals are included. We use here line widths for the hydrogenoid ions that include linear Stark broadening (Gonzalez et al. 1998); these were not available to GLAM.

Figure 5 shows  $\kappa_r F(A)/X_A$  for the elements C, Mg, Si, and Fe, calculated using three different methods: sampling, GLAM, and using Seaton's (1997) interpolation tables. This quantity is essentially independent of the stellar model used (i.e., it is independent of  $T_{\text{eff}}$ ,  $r$ , and the radius of the star) and is directly proportional to  $g_{\text{rad}}$ . Seaton (1997) already noticed a substantial difference between his results for Fe and earlier results obtained by LeBlanc & Michaud (1995) using the GLAM method. This is found again here. The differences between the GLAM-method and sampling results are not as large for the following reasons: (1) the same mixture of 11 elements and the same atomic data were used for both (Seaton [1997] also included the elements Na, Al, Ca, Cr, Mn, and Ni), and (2) fine structure was not included in either case. A large part of the difference between Seaton's results and the results of the sampling method can certainly be attributed to the inclusion of fine structure by Seaton; by splitting strong lines, fine structure reduces line saturation and thus increases overall absorption. In addition other factors such as different line widths and small variations in the equation of state can also contribute to the difference between the results of Seaton (1997) and those presented here.

Two other factors are important for Fe. Seaton (1997) used the Kurucz data for ions Fe I through Fe VI (Seaton, 2000, private communication), while we used the Kurucz data for only the first two ionization states of Fe. Moreover,

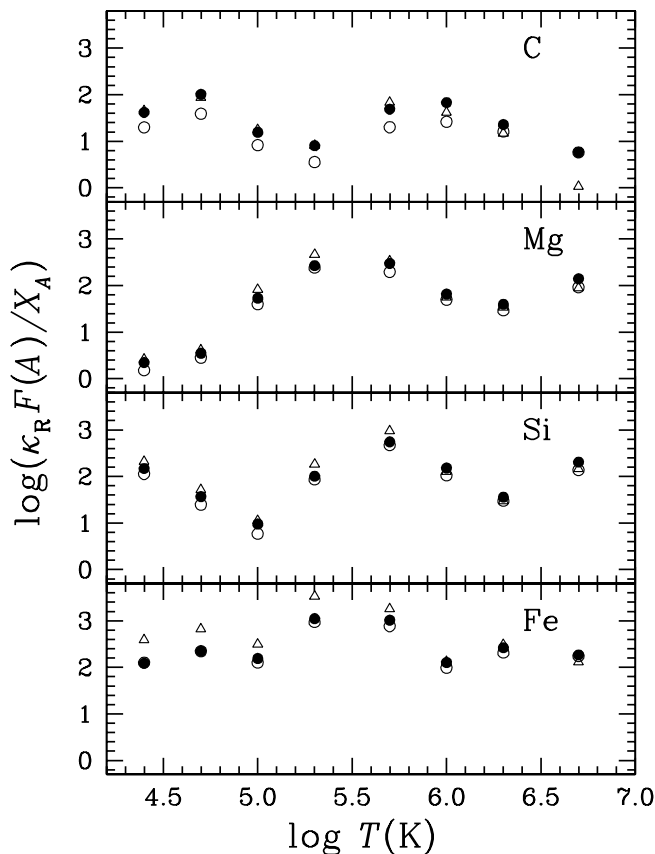


FIG. 5.—Model independent factor  $\kappa_r F(A)/X_A$  (in  $\text{cm}^2 \text{g}^{-1}$ ) for a solar abundance of the elements C, Mg, Si, and Fe using the sampling method discussed here (filled circles), the GLAM method (open circles), and Seaton's (1997) interpolation tables (triangles). In all these methods the diffusion coefficients of all ions of an element were supposed equal and electron recoil was neglected.

Seaton (1997) used the PLUS data (Lynas-Gray et al. 1995) for ions Fe VIII through Fe XIII, while it was not available to us. This, and his inclusion of fine structure, easily explains his higher  $g_{\text{rad}}(\text{Fe})$  values below  $T = 10^6$  K.

The  $g_{\text{rad}}$  obtained with the GLAM method are lower than those given by the sampling method throughout most of the stellar envelope. The reason is that for low temperatures (i.e., for Mg this corresponds to  $\log T \lesssim 5.5$ ; see Fig. 1) the line widths are narrower than frequency grid intervals. Thus the valleys in the background opacity spectrum are artificially filled because the line opacities are evenly distributed in the frequency intervals. This has the effect of blocking the flux more evenly as a function of frequency and it diminishes  $F(A)$ . Inversely, at the high core temperatures the GLAM method overestimates  $F(A)$  because the line widths become wider than the GLAM frequency intervals and valleys in the opacity spectrum are then artificially created<sup>3</sup> thus increasing the value of  $F(A)$ ; however this increase is generally offset by the fact that for  $\log T \gtrsim 6$ ,  $\kappa_r$  obtained by the sampling method are larger than those obtained using the GLAM method.

Comparisons with radiative accelerations obtained using OPAL data are shown in Figure 7 of Richer et al. (1998).

## 7. MOMENTUM REDISTRIBUTION

We have calculated correction factors (on the same temperature-pressure grid used in GLAM), which are simply the  $g_{\text{rad}}$  calculated by the GLAM method including the effect of the diffusion coefficients of the various ions (i.e., ion averaging; see eq. [15] of GLAM), redistribution, and electron recoil during photoionization, over the  $g_{\text{rad}}$  also calculated with the GLAM method but neglecting these effects, for the elements presented here. Many of the deficiencies of the GLAM-method calculations cancel out in such ratios and the resulting correction factors are expected to be accurate over a broader range than the GLAM-method  $g_{\text{rad}}$  themselves. The correction factors can be used to include these effects in calculations such as the sampling method, that leave them out.

Two sets of correction factors were calculated. In the first set, it was supposed that, for bound-bound transitions, if the excited level had a quantum number  $n$  larger than that of the fundamental level of the absorbing ion, the momentum was then spent in the next ionization state, i.e., the ion ionizes before having spent its acquired momentum; in the following, we will refer to that form of correction as “ $n_2 > n_1$  redistribution” for short. In the second set, if the excited level had a quantum number larger than that of the fundamental level plus one, we assumed that the momentum was transferred to the next ionization state; this will be referred to as “ $n_2 > n_1 + 1$  redistribution”. From these two calculations, one can estimate the uncertainty associated with our ignorance of what really happens, on average, after a photon is absorbed; to do better one should solve, for all ionization states, the full set of rate equations for all internal electronic transitions, including the various collision induced ones. Such calculations would be extremely difficult, which is why the two rough estimates given here are

<sup>3</sup> Recall that in the GLAM method, “background” lines have no wings; they are forced into a rectangular shape one frequency interval wide.

useful: they show clearly in what temperature range such calculation efforts will have to be concentrated in the future, and they show the order of magnitude of the corrections. The true results are expected to lie somewhere in between or near these two approximations (see GLAM for more details).

For photoionization we supposed that the momentum was spent in the newly acquired ionization state. The electron recoil formula used for all energy levels of the elements considered is that of the fundamental state of hydrogen (Sommerfeld 1939; see § 6 of GLAM for more details).

Figure 6 shows  $g_{\text{rad}}(\text{Si})$  in three different zero age main-sequence stellar models ranging from  $T_{\text{eff}} = 8000$  K to 14,000 K. Three curves are shown in each case. Dotted curves represent the  $g_{\text{rad}}$  given by Seaton (1997) using the same diffusion coefficient for the various ions and neglecting electron recoil. Dashed curves give the  $g_{\text{rad}}$  obtained using all correction factors just mentioned, with “ $n_2 > n_1$  redistribution”. The solid curves show the results with “ $n_2 > n_1 + 1$  redistribution”. The radiative accelerations are generally similar in all three models shown.

The diffusion coefficient correction is especially important in the stellar atmosphere where neutral ions are abundant. This is due to their high mobility compared to that of their singly charged ionic state. Michaud et al. (1979) have suggested, based on a detailed study of helium, that the

ratio of the diffusion coefficient of a neutral ion to that of a singly charged ion is of the order of 100. This makes  $g_{\text{rad}}$  particularly sensitive to the details of the redistribution mechanism. “ $n_2 > n_1 + 1$  redistribution” makes redistribution toward more ionized states less likely than with “ $n_2 > n_1$  redistribution” and thus favors the very rapidly diffusing neutral atoms; the increased mean diffusion velocity corresponds to an increased mean radiative force, as can be seen here. Since Si is less ionized in the cooler regions of the  $T_{\text{eff}} = 8000$  K model the effect of ion mobility is stronger there than in the 12,000 and 14,000 K models.

At very high temperatures the  $g_{\text{rad}}$  that include diffusion coefficients, redistribution, and electron recoil are smaller because continuum absorption begins to dominate and the momentum carried off by the electron becomes important (contributing negatively to  $g_{\text{rad}}$  at these temperatures). This conclusion may, however, depend on the approximate electron recoil formula used here.

These correction factors are available from the authors and were used in stellar evolution codes that include atomic diffusion (Richer et al. 1998; Turcotte et al. 1998a, 1998b).

The effect of the high mobility of the neutral ion and that of redistribution on  $g_{\text{rad}}$  can then be important in the atmospheres of Ap and HgMn stars where it is believed that radiative diffusion dominates other hydrodynamical processes. In AmFm stars an iron convection zone (Richer et al. 2000) seems to develop as a result of outward diffusion of iron peak elements, in which case the elements could separate much deeper in stars, near  $\log T \sim 5.3$ . In that case, all three calculations (see Fig. 6) are roughly equivalent.

## 8. CONCLUSION

We suggest the following number of frequency points for different temperature ranges be used for opacity calculations on nonuniform grids, if they are to be applied in evolutionary codes that include radiative diffusion: 50,000 points for  $4.20 \leq \log T \leq 4.5$ , 30,000 points for  $4.5 < \log T \leq 4.8$ , 10,000 points for  $4.8 < \log T \leq 5.5$ , and 4000 points for  $\log T > 5.5$ . These nonuniform frequency grids can be obtained from the authors or calculated with the method discussed in Appendix A. The existence of monochromatic opacity tables calculated on these frequency meshes would enable simultaneous calculations of radiative forces and Rosseland opacities, and would make it possible to study the effects of diffusion on the evolution of hot stars (e.g., HgMn stars), where convection zones may be thin and where a higher frequency resolution is needed to properly integrate the radiative acceleration equation just below the atmosphere. These opacity tables could also be used in Ap stars, where the strong magnetic fields might inhibit convection.

For  $\log T \lesssim 4.2$  the number of frequency points needed to obtain precise  $g_{\text{rad}}$  can be approximated from Figure 1. It should be noted that at these low temperatures the diffusion approximation for the flux is no longer valid and thus the radiative transfer equation must be solved to obtain the flux precisely. The problem becomes much more complex.

It was also shown that there can be differences in  $g_{\text{rad}}$  calculations using opacity sampling and the GLAM method used here that are inherent to the treatment of the background opacity. The GLAM method has the advantage of being able to incorporate redistribution and electron recoil effects, while the opacity sampling method is prefer-

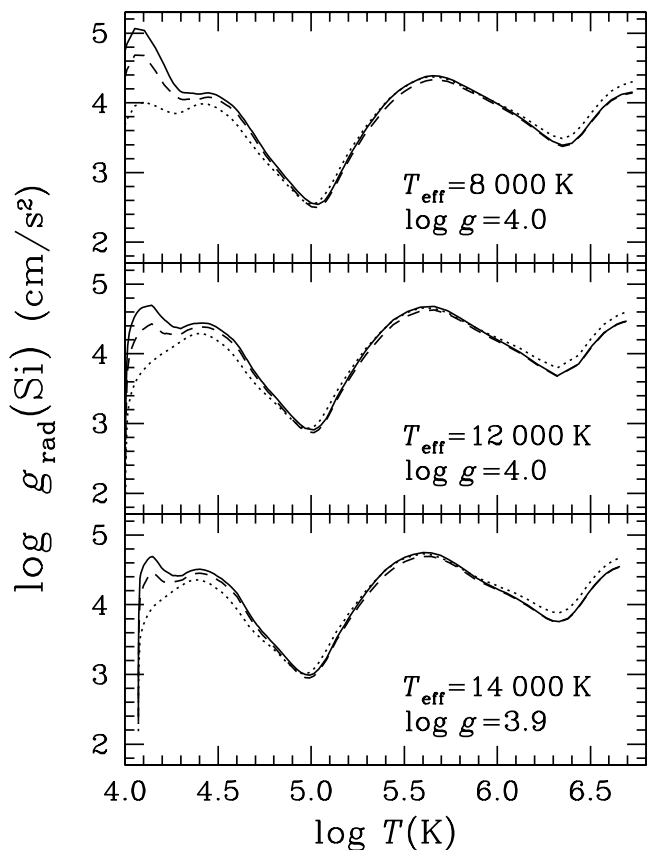


FIG. 6.—Radiative acceleration on a solar abundance of Si in different stellar models. The dotted curve is  $g_{\text{rad}}$  given by Seaton (1997) using the same diffusion coefficient for the various ions and neglecting electron recoil. The dashed curve results include the correction factors discussed in § 6, with “ $n_2 > n_1$  redistribution”; the solid curves suppose “ $n_2 > n_1 + 1$  redistribution”; both include electron recoil effects.

able for use in stellar evolution codes that incorporate atomic diffusion, since it can take into account the change to  $g_{\text{rad}}$  caused by the diffusion of the other species. The monochromatic opacities used to calculate  $g_{\text{rad}}$  by the sampling method can also be used to obtain  $\kappa_{\text{r}}$  during evolution.

Correction factors were calculated with the GLAM method; these may be used to include redistribution and electron recoil when using OPAL spectra as in Turcotte et al. (1998a, 1998b). It was shown that the inclusion of the diffusion coefficients and redistribution in the determination of  $g_{\text{rad}}$  is imperative, for at least some elements, in the

outer regions of stars. The momentum carried away by the electron during photoionization might also be important for certain elements deep in stars.

This research was partially funded by NSERC. F. L. would like to thank l'Association des universités partiellement ou entièrement de langue française (Fonds International pour la Coopération Universitaire) and the Faculté des Études Supérieures et de la Recherche de l'Université de Moncton for funding. We also wish to thank the referee, Dr. M. J. Seaton, for his helpful comments.

## APPENDIX A

### NONUNIFORM FREQUENCY GRID GENERATION

Our aim is to generate a  $M$ -point  $u$  grid such that for most of the grid we shall have

$$\mathcal{P}(u_i)(u_{i+1} - u_i) \approx 1/M, \quad (\text{A1})$$

where  $\mathcal{P}(u)$  is given by equation (2). This grid will then have the property that all intervals will carry roughly the same weight in integrations over the spectrum. We first define an auxiliary function  $\mathcal{Q}(u)$ , which is the integral of  $\mathcal{P}(u)$ ,

$$\mathcal{Q}(u) \equiv \int_0^u \mathcal{P}(u') du'. \quad (\text{A2})$$

Roughly speaking, the desired nonuniform grid is simply obtained by solving numerically each equation,

$$\mathcal{Q}(u_i) = i/M, \quad i = 1, 2, \dots, M, \quad (\text{A3})$$

for  $u_i$ . Of course, this cannot be the exact procedure since it would lead among other things, to an infinite  $u_M$  (at least in principle). One could replace  $i/M$  by  $i/(M+1)$  or generate  $M-1$  points instead of  $M$ , but this would still not lead to a satisfactory solution for another reason: we need to have grid points very close to the limits of our integration domain. The reason for this is that the line generation routine we used during our tests considered only those lines with  $u_1 < u_{\text{center}} < u_M$ ; since the wings of some lines (in particular H and He lines) can cover a wide part of the spectrum even when the line center is located at  $u \ll 1$ ,  $u_1$  has to be a tiny number. Because of the behavior of  $\mathcal{P}(u)$  for  $u \rightarrow 0$ , equation (A3) always yields values for  $u_1$  that are much too large (say,  $\sim 0.1$ ) even for  $M$  as high as  $10^5$ . We also want the upper limit  $u_M$  to be as nearly independent of  $M$ , and as close to 20 as possible, for simplicity, clarity, and ease of comparison with other integration methods; imposing  $u_M = 20$  would solve this problem, but this may violate equation (A1) for the last interval.

A simple solution to this boundary problem comes up naturally from the numerical method used to solve equations (A2) and (A3). So we now present the actual procedure used.

First we generate a  $N+1$  point uniform grid  $\tilde{u}_j$ , with  $N \gg M$ :

$$\tilde{u}_j = u_{\text{max}} \frac{j}{N}, \quad j = 0, 1, 2, \dots, N, \quad (\text{A4})$$

where we have selected  $u_{\text{max}} = 20$  for our work. Then we evaluate  $p_j \equiv \mathcal{P}(\tilde{u}_j)$  and pass the two series of numbers  $(\tilde{u}_j, p_j)$  to a cubic-spline fit routine that also performs an analytic integration of the resulting cubic-splines, yielding excellent approximations  $q_j$  to  $\mathcal{Q}(\tilde{u}_j)$  on the same uniform mesh (with  $q_0 = 0$ , identically). We then select the first interior points of the uniform grid,  $\tilde{u}_1$  and  $\tilde{u}_{N-1}$  as our nonuniform grid boundaries; more precisely, we select the corresponding  $\mathcal{Q}$  values  $q_1$  and  $q_{N-1} \equiv q_{\text{max}}$  as the limits for the linear ramp in equation (A3). The  $M$ -point nonuniform grid is then given by the solutions of the following equations:

$$\mathcal{Q}(u_i) = \frac{q_1(M-i) + q_{\text{max}}(i-1)}{M-1}, \quad i = 1, 2, \dots, M. \quad (\text{A5})$$

These are solved very efficiently by doing  $M$  cubic-spline interpolations over the set of data points  $(q_j, \tilde{u}_j)$ ,  $j = 0, \dots, N$  (note the pair reversal compared to the set used for spline integration). By including the limit points  $j = 0$  and  $j = N$  in the data set, we avoid numerical difficulties in computing  $u_1$  and  $u_M$  from the same formula; these turn out to be always very close to  $\tilde{u}_1 \sim 1/N \ll 1$ , and  $\tilde{u}_{N-1} \approx [1 - (1/N)]u_{\text{max}}$ , respectively.

The choice of the underlying uniform grid resolution is not very important, since its only use is to construct interpolation splines and fix the boundary points. We adopted the arbitrary relation  $N = 2M + 13$  for the grid calculations.

## REFERENCES

- Alecian, G. 1985, *A&A*, 145, 275  
 ———. 1994, *A&A*, 289, 885
- Alecian, G., & Artru, M.-C. 1990, *A&A*, 234, 323
- Alecian, G., Michaud, G., & Tully, J. 1993, *ApJ*, 411, 882
- Borsenberger, J., Michaud, G., & Praderie, F. 1979, *A&A*, 76, 287
- Borsenberger, J., Praderie, F., & Michaud, G. 1981, *ApJ*, 243, 533
- Cunto, W., Mendoza, C., Ochsenein, F., & Zeippen, C. J. 1993, *A&A*, 275, L5
- Gonzalez, J.-F., Artru, M.-C., & Michaud, G. 1995a, *A&A*, 302, 788
- Gonzalez, J.-F., LeBlanc, F., Artru, M.-C., & Michaud, G. 1995b, *A&A*, 297, 223 (GLAM)
- Gonzalez, J.-F., Stehlé, C., Artru, M.-C., & Massacrier, G. 1998, *A&A*, 330, 1120
- Grevesse, N., & Noels, A. 1993, in *Origin and Evolution of the Elements*, ed. N. Prantzos, E. Vangioni-Flam, & M. Cassé (Cambridge: Cambridge Univ. Press), 15
- Grevesse, N., Noels, A., & Sauval, A. J. 1992, in *Proc. First SOHO Workshop: Coronal Streamers, Coronal Loops, and Coronal and Solar Wind Composition* (SEE N93-31343 12-92; Annapolis: ESA), 305
- Hui-Bon-Hoa, A., Alecian, G., & Artru, M.-C. 1996, *A&A*, 313, 624
- Hummer, D. G., & Mihalas, D. 1988, *ApJ*, 331, 794
- Iglesias, C. A., & Rogers, F. J. 1995, *ApJ*, 443, 460  
 ———. 1996, *ApJ*, 464, 943
- Kurucz, R. L. 1990, in *Trans. IAU*, ed. D. McNally, Vol. XXB, IAU (Dordrecht: Kluwer), 168  
 ———. 1991, in *Stellar Atmospheres: Beyond Classical Models*, ed. L. Crivellari, I. Hubeny, & D. Hummer (Dordrecht: Kluwer), 441
- LeBlanc, F., & LeBlanc, S. É. 1999, *JRASC*, 93, 185
- LeBlanc, F., & Michaud, G. 1995, *A&A*, 303, 166
- Lynas-Gray, A. E., Seaton, M. J., & Storey, P. J. 1995, *J. Phys. B*, 28, 2817
- Massacrier, G. 1996, *A&A*, 309, 979
- Massacrier, G., & El-Murr, K. 1996, *A&A*, 312, L25
- Michaud, G. 1970, *ApJ*, 160, 641
- Michaud, G., Montmerle, T., Cox, A. N., Magee, N. H., Hodson, S. W., & Martel, A. 1979, *ApJ*, 234, 206
- Richer, J., Michaud, G., & Massacrier, G. 1997, *A&A*, 317, 968
- Richer, J., Michaud, G., Rogers, F. J., Iglesias, C. A., Turcotte, S., & LeBlanc, F. 1998, *ApJ*, 492, 833
- Richer, J., Michaud, G., & Turcotte, S. 2000, *ApJ*, 529, 338
- Rogers, F. J., & Iglesias, C. A. 1992a, *ApJS*, 79, 507  
 ———. 1992b, *ApJ*, 401, 361
- Seaton, M. J. 1987, *J. Phys. B*, 20, 6363  
 ———. 1997, *MNRAS*, 289, 700  
 ———. 1999, *MNRAS*, 307, 1008
- Seaton, M. J., Zeippen, C. J., Tully, J. A., Pradhan, A. K., Mendoza, C., Hibbert, A., & Berrington, K. A. 1992, *Rev. Mex. Astron. Astrofis.*, 23, 19
- Sommerfeld, A. J. W. 1939, *Atombau und Spektrallinien*, Vol. 2 (5th ed.; Braunschweig: F. Vieweg)
- Turcotte, S., Richer, J., & Michaud, G. 1998a, *ApJ*, 504, 559
- Turcotte, S., Richer, J., Michaud, G., Iglesias, C. A., & Rogers, F. J. 1998b, *ApJ*, 504, 539